Science Forum (Journal of Pure and Applied Sciences)

Journal Homepage: https://atbuscienceforum.com.ng/index.php/jpas

Sedimentological, Facies Architecture and Palaeoenvironmental Reconstruction of Ajali and Mamu Formations exposures in Iyale and Agbenema, Northern Anambra Basin, Nigeria

Balogun, R.A., Odoma, A.N, and Ayok, J.
Department of Geology, Federal University, Lokoja, Kogi State, Nigeria

Abstract

This study provides an integrated investigation of the sedimentology, facies architecture, and palaeoenvironmental evolution of the Ajali Sandstone and Mamu Formation in the northern Anambra Basin, southeastern Nigeria. Detailed fieldwork along the Iyale–Agbenema corridor combined stratigraphic logging, granulometric analysis, petrographic studies, and heavy mineral characterization with facies classification and palaeoenvironmental reconstruction. The Ajali Sandstone is composed predominantly of medium- to coarse-grained, poorly sorted quartz arenites, characterized by prominent cross-bedding, flaser structures, herringbone cross-stratification, and Skolithos burrows. Grain-size parameters, C–M patterns, and linear discriminant functions collectively indicate deposition in tidally influenced fluvial–deltaic systems, shaped by alternating phases of high-energy braided river discharge and nearshore marine reworking. Petrographic evidence, complemented by heavy mineral assemblages enriched in zircon, tourmaline, and rutile, suggests high textural maturity and points to multicycle sediment recycling sourced from uplifted basement complexes and recycled sedimentary terranes. In contrast, the Mamu Formation is dominated by laminated clays, siltstones, shales, and ferruginised horizons bearing root traces and plant debris. These facies reflect deposition within lower delta plain to prodelta environments, marked by fluctuating redox conditions, quiet-water sedimentation, and episodic subaerial exposure. Together, the Ajali–Mamu successions capture the complex interplay of Late Cretaceous transgressive–regressive cycles in southeastern Nigeria, where proximal braided fluvial systems repeatedly prograded into coastal plain and shallow marine environments. The integration of sedimentological, petrographic, and provenance data highlights this succession as a key stratigraphic archive for reconstructing basin evolution, sediment dispersal pathways, and palaeoenvironmental dynamics within the Benue Trough system. Overall, these findings refine existing depositional models and underscore the controlling role of tidal–fluvial interactions in shaping the sedimentary architecture of paralic basins during the Late Cretaceous.

Keywords
Facies Architecture,
Palaeoenvironment,
Ajali Formation,
Mamu Formation,
Anambra Basin

Corresponding Author: Balogun, R.A, Department of Geology, Federal University, Lokoja, Kogi State, Nigeria.
Email: balogunr88@gmail.com

Introduction

The Anambra Basin, situated at the southern end of the Benue Trough, represents a major Upper Cretaceous–Palaeocene depocentre filled with thick siliciclastic successions that record significant tectono-sedimentary and palaeoenvironmental histories (Wright et al., 1985; Akande & Erdtmann, 1998; Obaje et al., 1999). Stratigraphically, the basin is bounded to the north by the Benue Trough and to the south by the Niger Delta, and it preserves a succession of Campanian to Maastrichtian sediments, including the Ajali Sandstone and the Mamu Formation, which remain crucial for basin analysis and hydrocarbon evaluation (Obaje et al., 2004; Anyiam et al., 2015).

Sedimentological studies in the basin have provided insights into depositional environments, provenance, and basin evolution, with facies analysis playing a key role in palaeoenvironmental reconstruction (Dim et al., 2018; Adamu et al., 2017;2018a; b; c;2020; 2022aYusuf et al., 2023). However, despite numerous contributions, detailed sedimentological and facies-based reconstructions of the Ajali and Mamu Formations in the northern sector, particularly around Iyale and Agbenema, remain sparse. This knowledge gap has been attributed to poor exposure, inadequate field mapping, and limited integration of facies architecture with provenance and palaeoenvironmental data (Obaje et al., 2020; Adamu et al., 2022b).

Understanding the depositional systems of these units is critical not only for reconstructing palaeoenvironments but also for evaluating reservoir quality and hydrocarbon potential in Nigeria's inland basins, where subsurface data are limited (Magoon & Dow, 1994; Obaje et al., 2013). Surface-based sedimentological and petrographic analyses therefore provide an essential framework for constraining reservoir characteristics, source-to-sink relationships, and petroleum system elements. This study investigates the sedimentology, facies associations, and palaeoenvironmental evolution of the Ajali and Mamu Formations in Iyale and Agbenema. By integrating field-based lithofacies description, granulometric, and heavy mineral analyses, the research aims to refine depositional models for the northern Anambra Basin, thereby contributing to regional stratigraphic understanding and hydrocarbon prospectivity assessment.

Stratigraphy of the Anambra Basin

The stratigraphic framework of the Anambra Basin records a complex tectono-sedimentary evolution associated with Santonian orogenic movements in West Africa. During the mid-Santonian, widespread tectonic activity led to the uplift and folding of pre-Santonian sediments, forming the Abakaliki anticlinorium and accompanied by localised volcanic intrusions in the Abakaliki area (Guiraud & Bosworth, 1997). Subsidence adjacent to this uplift created two principal depocentres: The Afikpo Syncline to the southeast and the much larger Anambra Basin to the northwest (Fig. 1).

These structural reorganisations marked a major palaeogeographic shift, transforming the Anambra Basin into the principal repository for Upper Cretaceous clastics (Zaborski, 2000). The stratigraphy of the basin is dominated by Campanian to Palaeocene sediments, deposited in alternating transgressive and regressive phases (Nwajide & Reijers, 1996). The basal succession is represented by the Nkporo Group, comprising the Nkporo Shale and its lateral equivalents, the Enugu and Owelli Formations. These units are predominantly marine shales interbedded with deltaic sandstones and carbonaceous horizons, and often display siderite and pyrite mineralisation indicative of early diagenetic processes (Odumoso et al., 2013).

Overlying the Nkporo Group is the coal-bearing Mamu Formation of Maastrichtian age. This unit reflects deposition in deltaic plain and swamp environments, characterised by cyclic alternations of shales, sandy shales, and carbonaceous beds, with economic coal seams locally preserved (Whiteman, 1982; Nwajide, 2013). Its facies associations indicate fluctuating conditions between fluvial-deltaic and shallow marine settings. The Ajali Sandstone, also Maastrichtian, conformably overlies the Mamu Formation. It consists predominantly of cross-bedded, medium- to coarse-grained sandstones with subordinate clay interbeds, interpreted as fluvio-deltaic channel and shoreface deposits (Fatoye & Yomi, 2013). This formation represents one of the most significant reservoir-prone units in the basin, often displaying textural maturity and high porosity.

The Nsukka Formation, of Danian age, caps the succession. It comprises alternating sandstones, sandy shales, plant-rich beds, and thin coals, deposited in a fluvial-deltaic environment during a period of reduced marine influence (Reyment, 1965; Agagu et al., 1985). This formation bridges the transition from Cretaceous to Palaeogene sedimentation and records the early stages of proto-Niger Delta development (Obaje et al., 2004; Erepamo et al., 2022).

Overall, the stratigraphy of the Anambra Basin illustrates a dynamic depositional history, controlled by tectonics, eustasy, and sediment supply, with significant implications for reservoir distribution and hydrocarbon prospectivity (Ogumagbe et al., 2022; Alege et al., 2023).

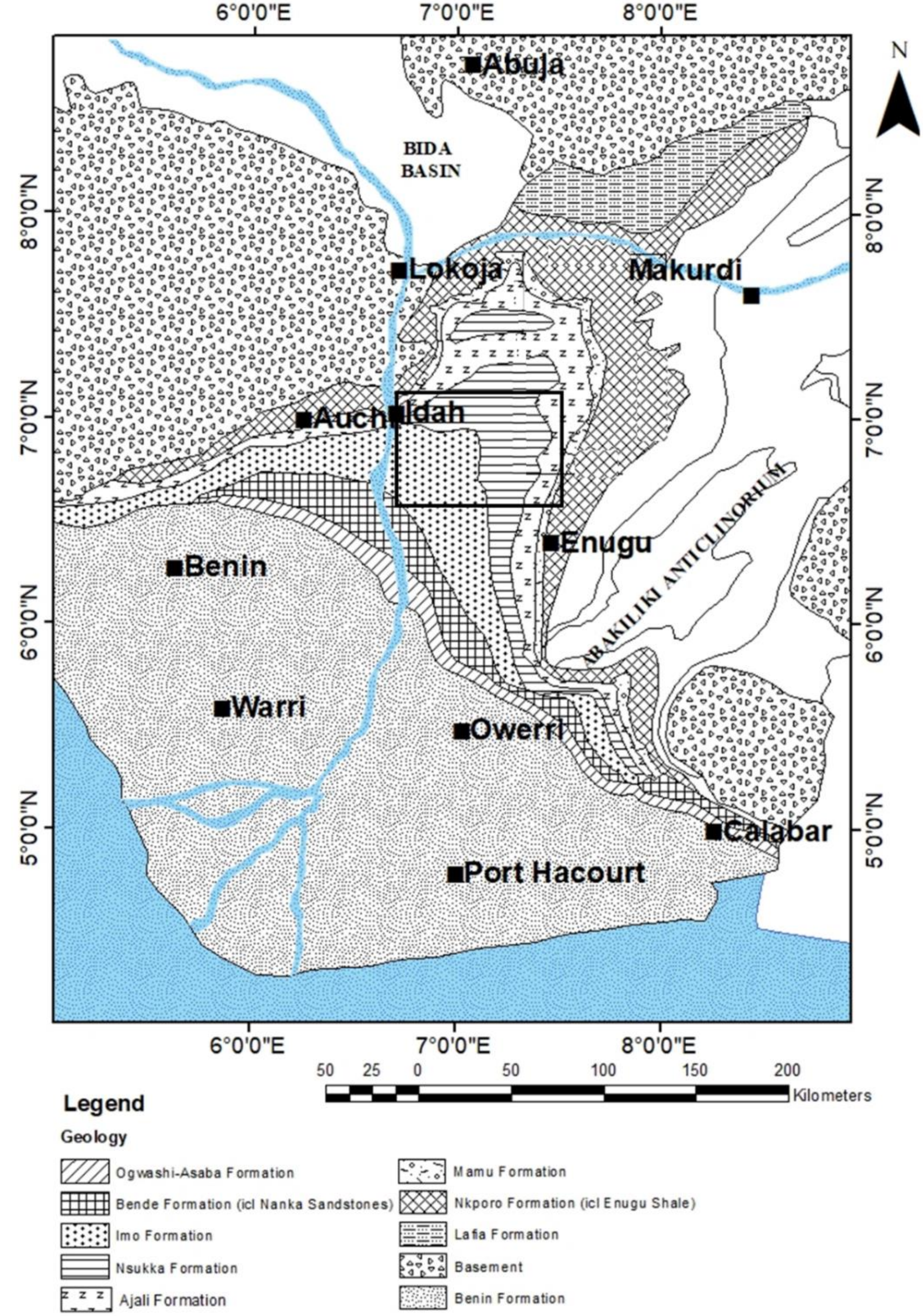

Figure 1. Regional Geology and stratigraphy of the southern Nigeria showing location of study site (modified from Obaje, 2009).

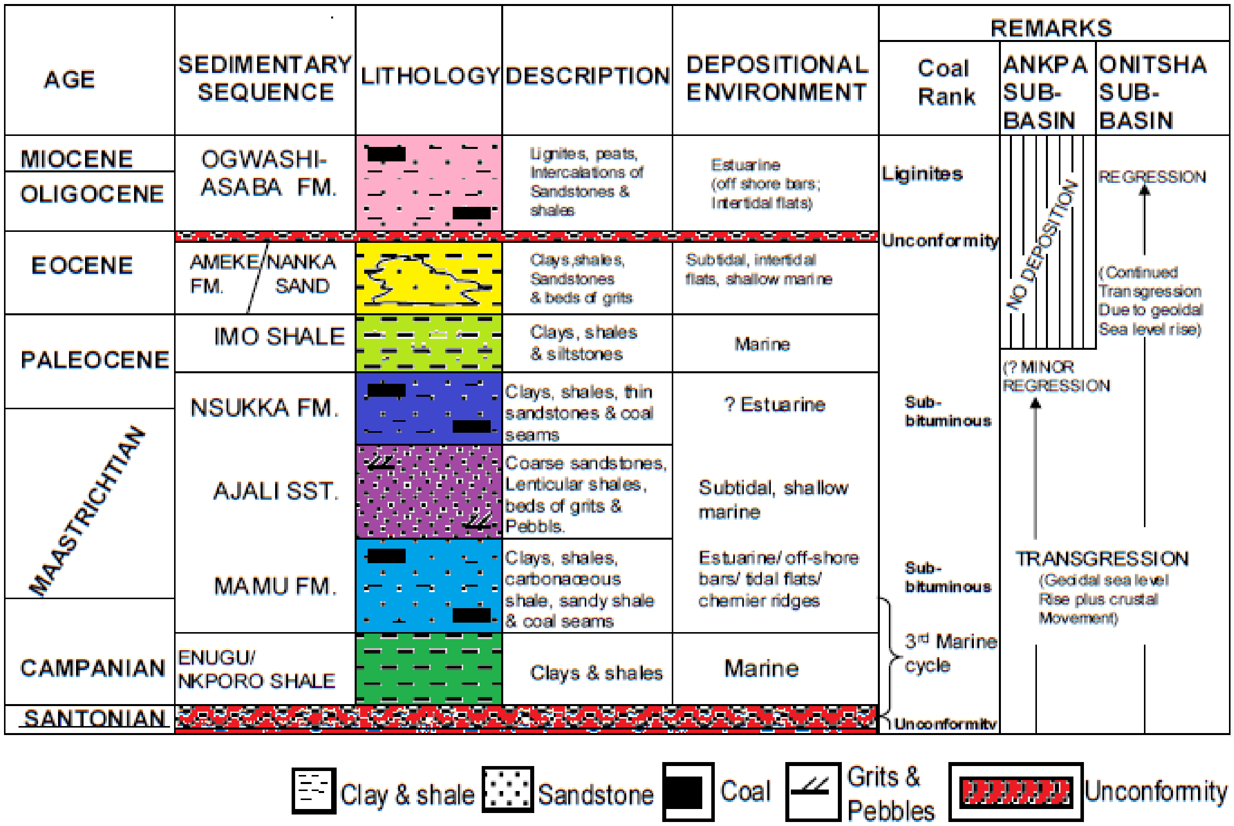

Figure 2. Generalised stratigraphic succession of the Anambra Basin showing the Nkporo, Mamu, Ajali, and Nsukka Formations

Methods

Detailed fieldwork was undertaken across the Iyale–Agbenema corridor in the northern Anambra Basin to investigate the sedimentology, facies architecture, and palaeoenvironmental framework of the Ajali Sandstone and Mamu Formation. Traverses were conducted along major roads, minor footpaths, and stream-cut exposures where lithological units were most clearly displayed. Geographic coordinates and directional bearings were recorded using a Garmin GPS and a Brunton compass. Stratigraphic sections were logged systematically, with observations on lithology, texture, colour, sedimentary structures, fossil content, and bed geometry. Weathered horizons were avoided to ensure representative sampling. A total of 25 fresh samples were collected, including 20 from the Ajali Sandstone at Iyale and 5 from the Mamu Formation at Agbenema. Each sample was labelled with location, stratigraphic position, and lithological description. Field sketches and photographic documentation were also undertaken for correlation of facies units.

Granulometric analyses were conducted on the Ajali Sandstone samples using standard dry sieving techniques (Blott & Pye, 2001). Grain-size statistical parameters; mean, sorting, skewness, and kurtosis were computed following the logarithmic graphical method of Folk and Ward (1957). These data were further employed in multivariate discriminant approaches, including Linear Discriminant Functions (LDFs) and the C–M diagram (Passega, 1964), to infer depositional environments.

Thin sections were prepared from selected sandstone samples and examined under a polarising microscope to determine textural maturity, mineralogical composition, and diagenetic features. Heavy mineral analyses were carried out on fine to very fine sand fractions (125–63 µm) to ensure enrichment of diagnostic heavy minerals (Morton & Hallsworth, 1999). Heavy minerals were separated using bromoform (specific gravity 2.89 g/cm³) and mounted for petrographic identification with a binocular microscope. The Mamu Formation samples were analysed for lithofacies characterisation, with emphasis on vertical facies successions, coal–shale alternations, and palaeoenvironmental indicators such as root traces and plant debris. Facies classification followed the scheme of Miall (1996), enabling interpretation of depositional processes and palaeoenvironmental settings.

All laboratory analyses were conducted at the Sedimentology Laboratory, Department of Earth Sciences, Prince Abubakar Audu University, Anyigba, and at the Department of Geology, Ahmadu Bello University, Zaria.

4. Results and Discussion

4.1 Location Analysis

4.1.1 Ajali Sandstone Exposed in Iyale and Environs

The Ajali Sandstone forms prominent exposures along the Abejukolo–Anyigba road corridor in Iyale, displaying a thickness of approximately 7 m at the basal section. The lower part comprises white, coarse-grained, poorly sorted, negatively skewed, leptokurtic sandstone dominated by parallel cross-bedding. This unit is succeeded by tabular cross-bedded, well-sorted, coarse-grained sandstone with similar skewness and kurtosis parameters, indicating rapid sediment transport under high-energy conditions.

Overlying this is a 6 m thick, medium-grained sandstone, moderately sorted, strongly fine-skewed and very platykurtic, which reflects waning flow conditions. The succession continues upward into coarse-grained, poorly sorted, negatively skewed, platykurtic sandstones capped by ferruginised, medium-grained units, again poorly sorted and mesokurtic (Figs. 3a–c and 4). Moving eastward along the Abejukolo road, a low-relief exposure displays alternating white and ferruginised sandstones separated by reactivation surfaces. Herringbone cross-bedding and parallel lamination dominate the section, with basal medium-grained, moderately sorted, mesokurtic facies passing upward into coarse, poorly sorted platykurtic sandstones.

The alternation of white and ferruginised beds reflects fluctuating oxidation and diagenetic conditions. The strong coarse skewness across these facies points to a high-energy depositional setting with periodic tidal reworking (Fig. 3c). Approximately 1 km further east, a sandstone excavation site exposes stratified successions bearing skolithos burrows (Skolithos ichnofacies). These biogenic structures suggest colonisation in a high-energy shallow marine setting (Pemberton & MacEachern, 1997). The basal units are poorly sorted, platykurtic sandstones overlain by mesokurtic sandstone and capped by moderately sorted, platykurtic sandstone, all medium- to coarse-grained. The overall stacking indicates repeated episodes of energetic deposition punctuated by bioturbation.

To the northwest of Iyale, the lithological section begins with a 3 m thick, white, coarse-grained, moderately sorted, tabular cross-bedded sandstone. Clast shapes vary from angular to well rounded, reflecting mixed provenance and transport histories. This is overlain by a 0.7 m thick alternation of red and white, poorly sorted, flaser cross-bedded coarse sandstone, succeeded by a 1.8 m thick, herringbone cross-bedded sandstone containing angular to subangular clasts and pebbly basal lag deposits (Fig. 3c). The presence of clay lenses and upward fining within this interval signifies fluctuating flow conditions typical of tidal channels. Higher up, a ferruginised, flaser cross-bedded sandstone rests on a friable, dirty red sandstone, while the section terminates with medium-grained, tabular cross-bedded sandstone capped by lateritised horizons (Fig. 4). Collectively, the Ajali Sandstone exposures reveal strong evidence of tidally influenced fluvial processes. The recurrence of herringbone and flaser bedding, reactivation surfaces, wave ripples, and Skolithos burrows confirm the alternating influence of bidirectional tidal currents and episodic subaerial exposure. The ferruginisation is linked to post-depositional oxidation during periodic emergence, a feature commonly reported in Upper Cretaceous deltaic to marginal marine settings (Nwajide, 2013; Obi et al., 2020).

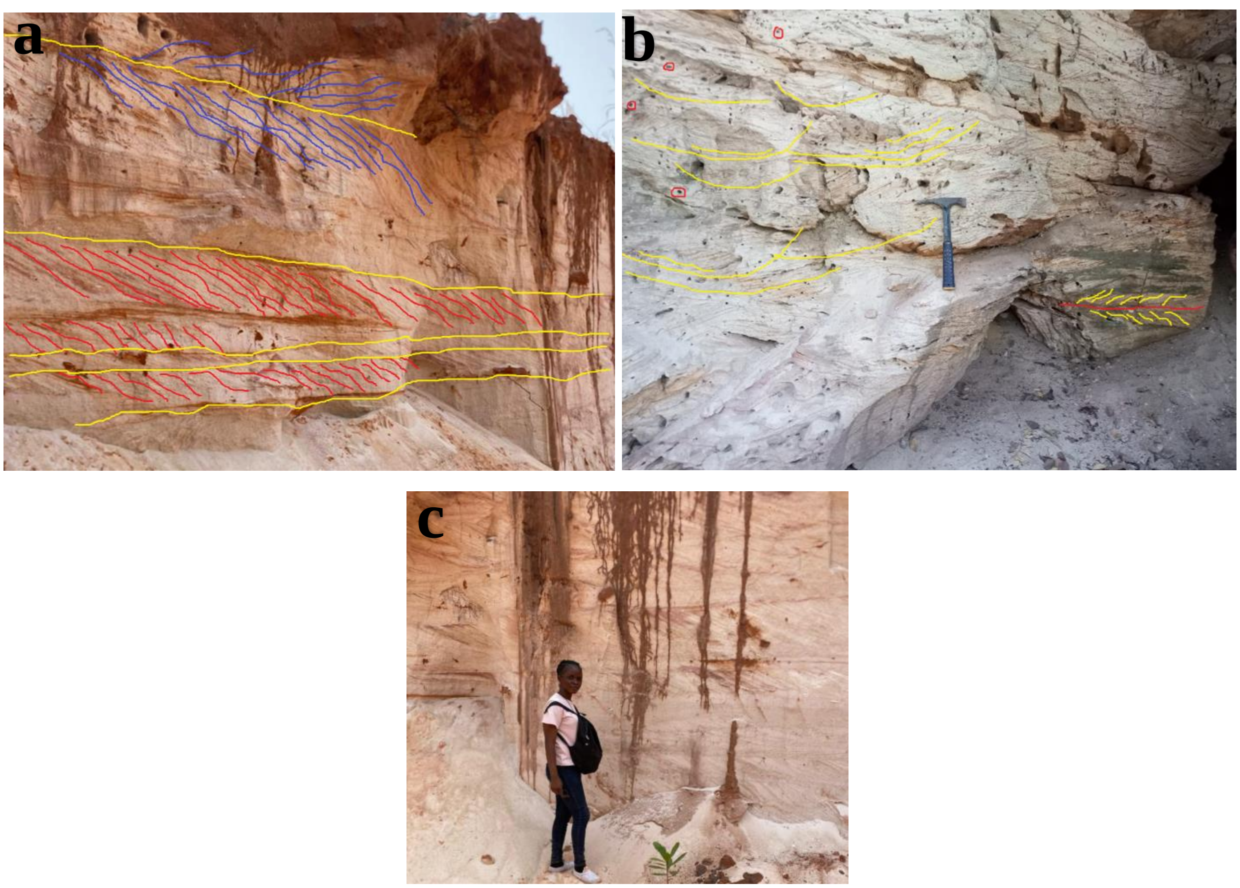

Figure 3. Exposed sections of Ajali Formation at Iyale: (a) quarry with cross-bedding and clay bands; (b) road section with herringbone, trough, flaser cross-beds and Skolithos burrows; (c) excavation site with tabular cross-bedding and ichnofossils.

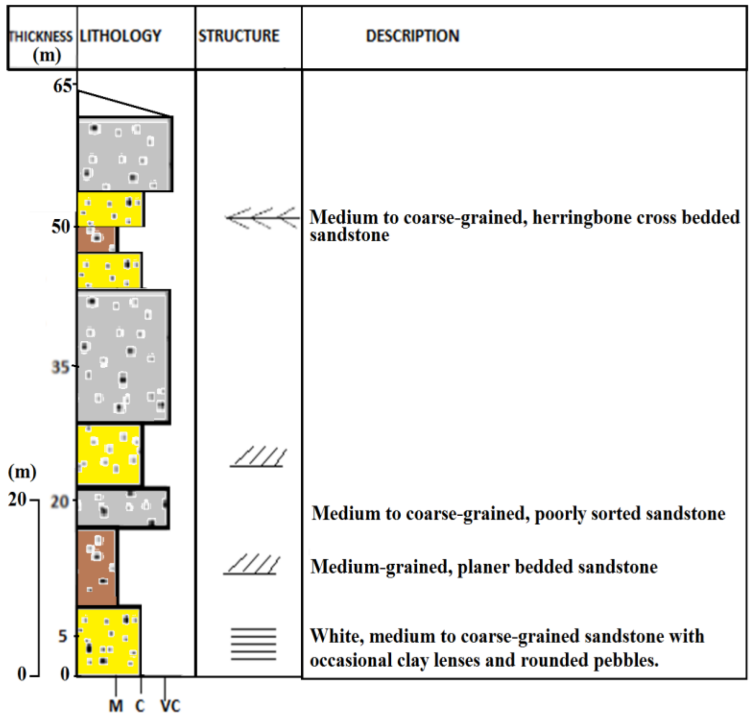

Figure 4. Composite lithological log of Ajali Sandstone at Iyale (N07°38'11.04"N, 007°20'33.42"E).

Facies Analysis of the Ajali Sandstone

Nine lithofacies were recognised based on lithology, grain size, sedimentary structures, and trace fossils:

Massive Sandstone (Facies A): Alternating red and white, medium-grained, poorly to moderately sorted sandstones, massive in appearance, suggestive of rapid deposition under high-energy flow (Tucker, 1996).

Tabular Cross-Bedded Sandstone with Reactivation Surfaces (Facies B): Evidence of bidirectional flow regimes consistent with tidal sand waves (Boggs, 1995).

Trough Cross-Bedded Sandstone (Facies C): Medium- to fine-grained with clay drapes, reflecting tidal dune migration (Reading, 1996).

Herringbone Cross-Bedded Sandstone (Facies D): Classic tidal current indicator, reflecting alternating ebb- and flood-tide deposition (Allen, 1984).

Sandstone with Skolithos/Ophiomorpha Burrows (Facies E): Diagnostic of Skolithos ichnofacies, indicating marginal marine intertidal flats (Pemberton & MacEachern, 1997).

Well-Bedded Tabular Cross-Bedded Sandstone (Facies F): Deposited by migrating sand waves under oscillatory high-energy flow.

Cross-Bedded Sandstone with Wave Ripples (Facies G): Vertical transition into finer units, reflecting regressive tidal settings (Reineck & Singh, 1980).

Pebbly Sandstone (Facies H): Channel lag deposits, fining upwards, reflecting fluvial-tidal interaction.

Flaser-Bedded Sandstone (Facies I): Alternations of sand and mud drapes, typical of tidal flats and delta fronts (Tucker, 1996).

Facies Associations and Depositional Settings

FA-1: Subtidal Channel Association (Facies A, B, C, D, G, H, I):

Coarse-grained sandstones with herringbone and trough cross-bedding, reactivation surfaces, and pebble lags. These features point to tidal channels influenced by alternating marine and fluvial currents (Allen, 1984; Boggs, 1995).

FA-2: Intertidal Flat Association (Facies B, C, E, F, I):

Fining-upward sequences, Skolithos burrows, and flaser bedding indicate intertidal flats subjected to fluctuating hydrodynamic energy. Biogenic traces confirm oxygenated sandy substrates colonised by infauna (Pemberton & MacEachern, 1997).

The Ajali Sandstone thus represents a tidally influenced fluvial–deltaic system with repeated subtidal channel and intertidal flat deposits, shaped by alternating high-energy currents and periodic emergence.

4.1.2 Mamu Formation exposed in Agbenema area

Four distinct outcrops of the Mamu Formation were studied around Agbenema and Ofejiji, each logged in detail and labelled L1a–L2 (Table 4.1). These outcrops provided insights into lithological variability, sedimentary structures, and depositional architecture within the northern Anambra Basin.

Location 1a (N07° 47′ 50.88″, E007° 27′ 09.82″)
Exposures occur along the Omala–Anyigba road at Agbenema-Ife, extending over ~400 m. A composite thickness of 40 m was measured, comprising alternating grey silty clay, siltstones, and shales (Fig. 5a–b). The shales, predominantly calcareous, exhibit fissility with laminae 0.45–1.00 mm thick and frequent bioturbation. Beds trend NE–SW with local dips of 020°/10° SW. Siltstones are well laminated (0.50–1.50 m), while silty clays range 0.40–2.00 m.

Location 1b (N07° 47′ 47.72″, E007° 27′ 07.44″)
At the eastern part of Agbenema-Ife, a ~70 m long section was logged (Fig. 6a–b). The 10 m-thick interval is dominated by siltstones, light grey to yellow in colour, with well-developed bedding (1.00–2.00 m). Beds trend NE–SW with dips of 020°/8° SW. Laminations and bedding were the principal structures recorded.

Location 1c (N07° 47′ 57.77″, E007° 27′ 13.06″)
Exposures along Agbenema–Iyale road revealed 32 m of predominantly clay-rich successions (Fig. 7a–b). The clays, light grey to milky white, are finely laminated and bedded, ranging from 0.50–3.00 m in thickness. Bedding trends NE–SW with dips of 022°/7° SW.

Location 2 (N07° 45′ 13.55″, E007° 25′ 13.82″)
At Ofejiji, ~400 m of section was exposed along the township road (Fig. 8a–b). A total thickness of 300 m was logged, dominated by grey silty clay and shale. Shales are fissile (laminae 0.50–0.90 mm), while siltstones are massively laminated and intercalated with ferruginised silty clay. Clay units (2.00–10.0 m) dominate, with shales (1.50–3.00 m) interbedded. Bedding trends NE–SW with dips of 020°/10° SW. An angular unconformity was also noted, reflecting local tectonic reorganisation.

Overall, the exposures illustrate alternating shale–siltstone–clay successions, consistent with floodplain to deltaic settings within a shallow marine-influenced coastal plain, typical of the Maastrichtian Mamu Formation (Nwajide, 2013; Odumoso et al., 2013; Akande et al., 2021).

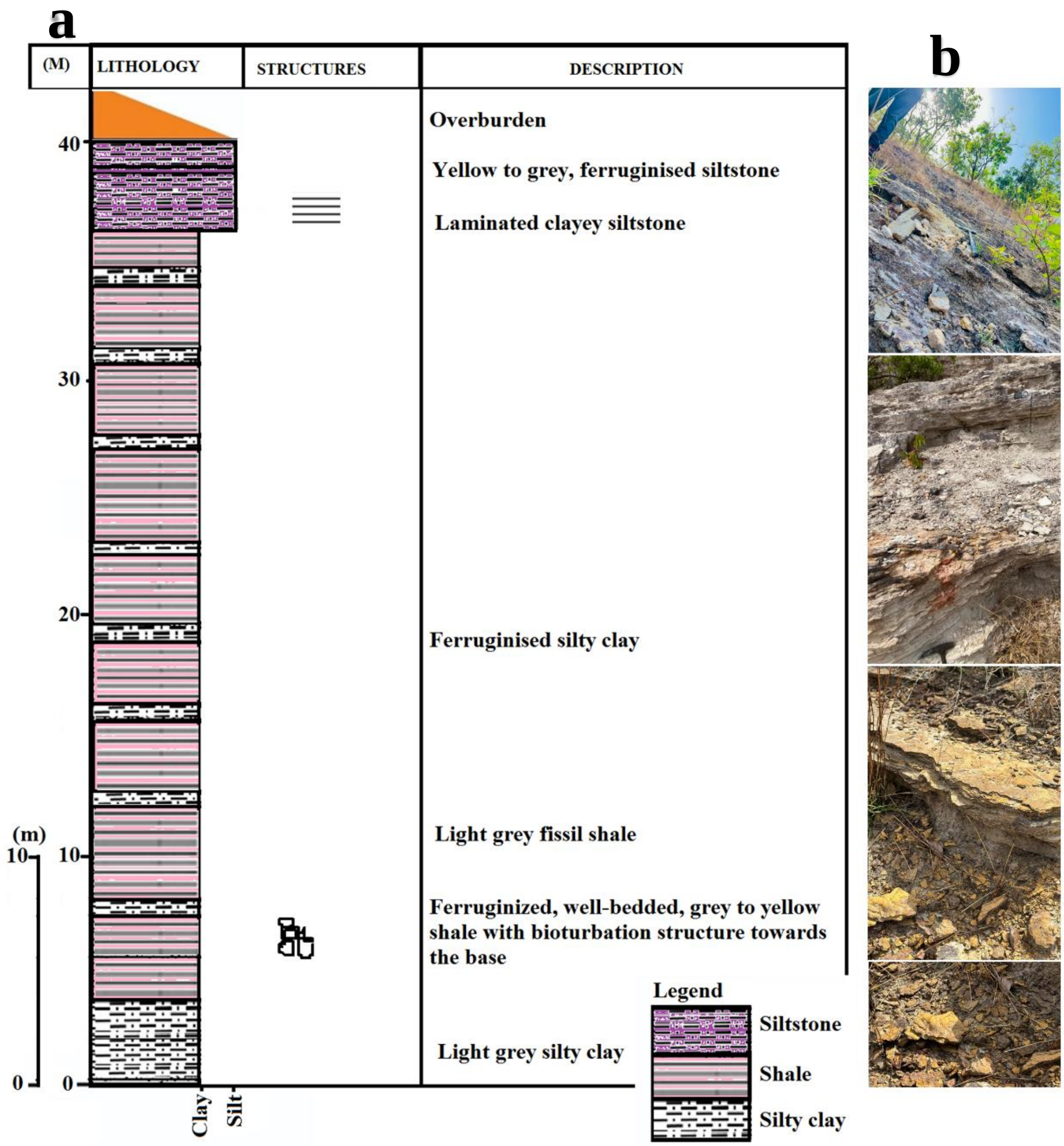

Figure 5. (a) Lithologic log (b) Exposed Section of exposed Section of Mamu Formation in Agbenema-Ife (N07° 47' 50.88", E007° 27' 09.82")

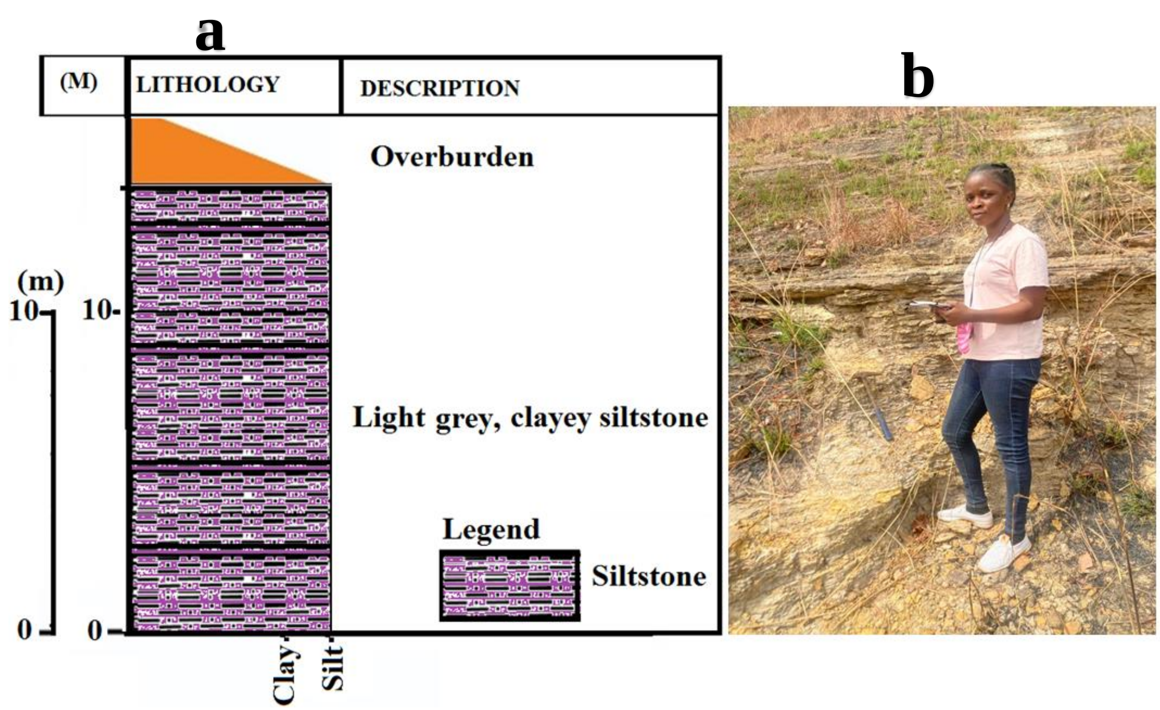

Figure 6. (a) Lithologic log (b) exposed Section of exposed Section of Mamu Formation in the eastern part of Agbenema-Ife town, Kogi State, Northcentral Nigeria (N07° 47' 47.72", E007° 27' 07.44")

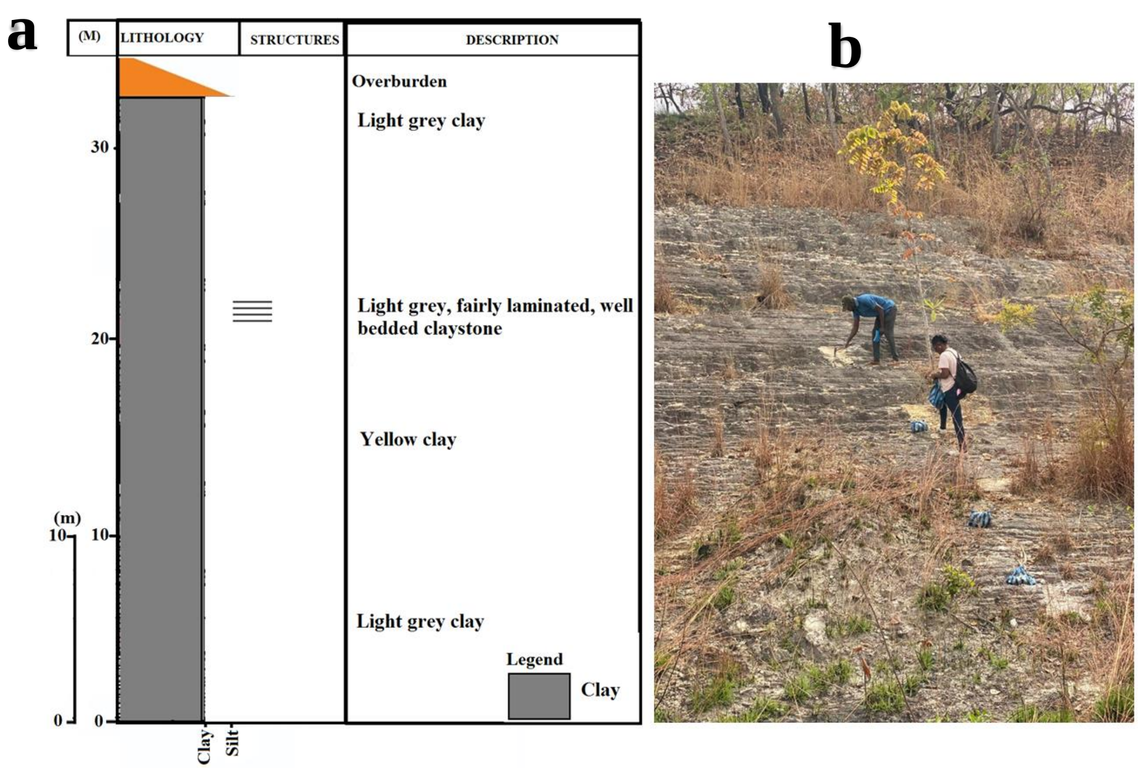

Figure 7. (a) Lithologic log (b) exposed road section of exposed Section of Mamu Formation along Agbenema-Iyale express way, Kogi State, Northcentral Nigeria (N07° 47' 57.77", E007° 27' 13.06")

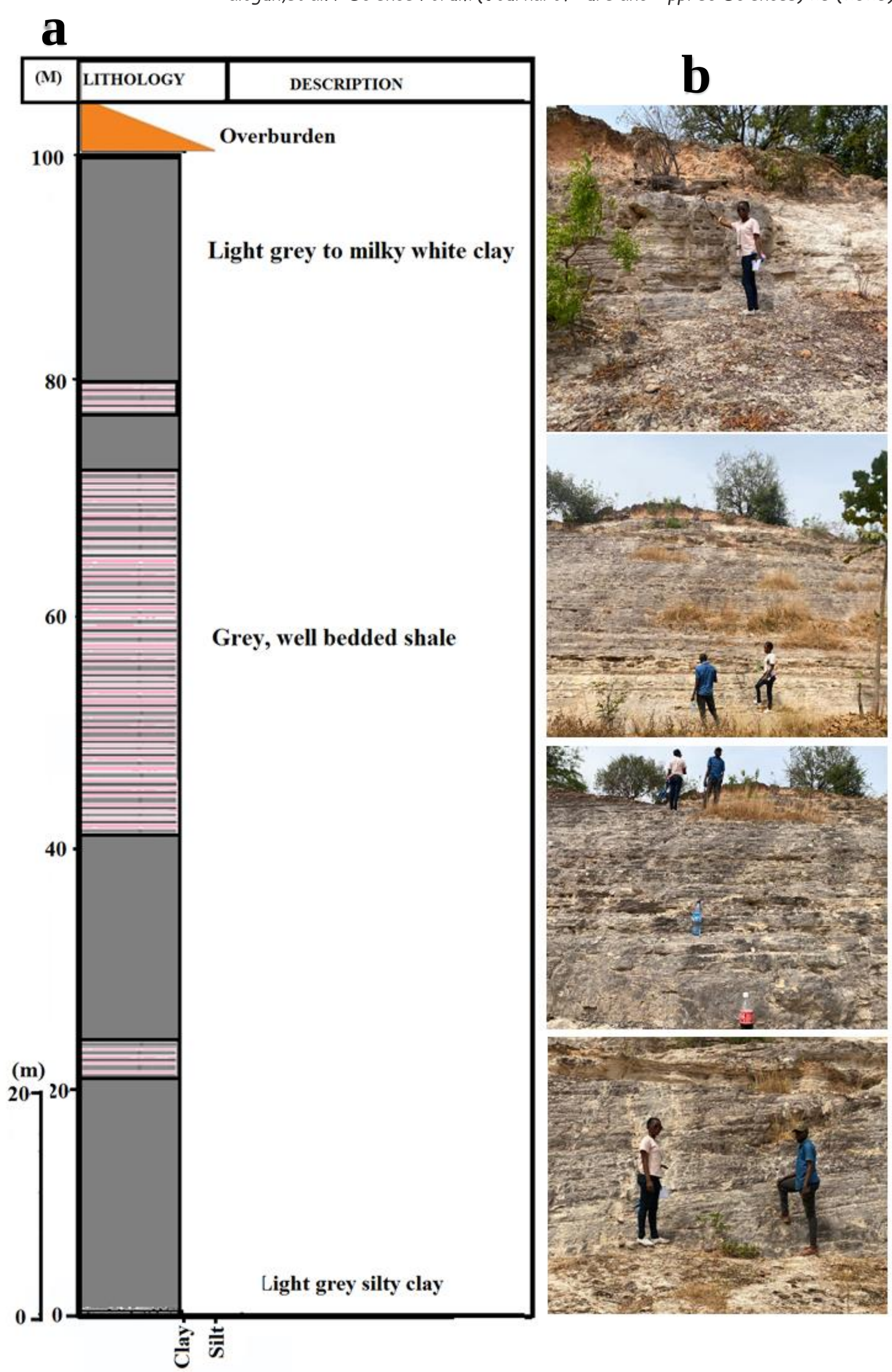

Figure 8. (a) Lithologic log of exposed Section of Mamu Formation, (b) exposed section of Mamu Formation along Anyigba-Omala road, Ofejiji town, Kogi State, Northcentral Nigeria (N07° 45' 13.55", E007° 25' 13.82")

Facies Analysis of the Mamu Formation
Four lithofacies were defined:

Clayey Siltstone (F1): Grey, fine to medium, laminated, with bioturbation and plant impressions, deposited under low–moderate energy.

Ferruginised Siltstone (F2): Reddish to mottled, with iron nodules and root traces, reflecting diagenetic alteration during subaerial exposure.

Clay (F3): Soft, plastic, organic-rich, deposited in floodplain ponds or interdistributary bays under dysoxic conditions.

Shale (F4): Dark grey to black, fissile, with pyrite nodules, deposited in anoxic prodelta/lagoonal settings.

Facies Associations and Depositional Settings

Lower Delta Plain Association (F1–F2): Alternations of siltstone and ferruginised units reflect seasonal waterlogging and oxidation.

Delta Front to Prodelta Association (F3–F4): Laminated clays and organic-rich shales indicate quiet-water deposition under marine influence.

The Mamu Formation records a deltaic depositional system, transitioning from lower delta plain to prodelta. Cyclic alternations of siltstone, shale, and ferruginised clay highlight fluctuating redox states, reflecting both fluvial and marine influences during the Late Campanian–Maastrichtian (Obaje, 2009; Mode et al., 2019). The Ajali and Mamu Formations in the northern Anambra Basin collectively document a tidally influenced fluvial–deltaic system. The Ajali Sandstone reflects high-energy subtidal channels and intertidal flats shaped by tidal reworking, while the Mamu Formation captures quieter delta plain to prodeltaic settings with evidence of oxidation, flooding, and organic matter preservation. Together, they provide robust palaeoenvironmental evidence for Late Cretaceous transgressive–regressive cycles in southeastern Nigeria.

4.2 Granulometric Studies

Grain size analysis provides an essential tool for interpreting depositional processes, sediment transport dynamics, and facies architecture in siliciclastic successions. The average grain size in a deposit reflects the prevailing energy regime, with particle sorting and distribution controlled by hydraulic conditions and provenance (Folk & Ward, 1957; Friedman, 1979). In the present study, granulometric data were derived from Ajali Sandstone and Mamu Formation exposures in Iyale and Agbenema, respectively. The results are presented in Tables 1 – 3, while the associated statistical plots are illustrated in Figure 9.

4.2.1 General Grain Size Distribution

The Ajali Sandstone samples from Iyale show grain sizes ranging from medium to coarse sand, with modal peaks between 0.20ϕ and 1.60ϕ. According to the Wentworth (1922) scale, this corresponds to medium–coarse grained sands (Table 4.1). The dominance of coarse fractions suggests deposition under relatively high-energy conditions typical of fluvial and shoreface systems, where competence and capacity of currents are sufficient to transport and winnow finer particles (Boggs, 2012). Conversely, samples from the Mamu Formation tend to be finer, with higher silt and clay admixtures, reflecting comparatively lower-energy depositional settings.

Table 1. Percnetile value from cumulative curve plots of Ajali Formation sandstones in Iyale area

Sample ID	(ϕ)5	(ϕ)16	(ϕ)25	(ϕ)50	(ϕ)75	(ϕ)84	(ϕ)95
RIY 1A	-1.52	-0.69	0.00	0.79	1.41	1.69	2.52
RIY 1B	-0.91	0.00	0.40	1.01	1.48	1.75	2.40
RIY 1C	-0.21	0.30	0.58	1.19	1.74	1.98	2.40
RIY 1D	-0.82	-0.11	0.32	1.09	1.58	1.98	2.59
RIY 1E	-0.61	0.21	0.39	1.19	1.78	2.21	2.73
RIY 3E	-0.22	0.41	0.59	1.27	1.78	2.13	2.53
RIY 3B	-1.01	-0.59	-0.25	0.76	1.60	1.78	2.53
RIY 3D	-0.81	0.10	0.28	1.02	1.61	2.00	2.29
RIY 4A	-1.72	-0.79	-0.25	1.02	1.78	2.09	2.50
RIY 4B	-0.91	-0.31	0.00	0.78	1.42	1.79	2.44

4.2.2 Univariate Grain Size Parameters

Graphic mean values (Mz) calculated after Folk and Ward (1957) reveal that Ajali Sandstone samples are dominantly coarse grained (e.g., RIY A, RIY B, RIY 3B), while others fall within medium grain size classes (RIY 1C, RIY 1E, RIY 3E). The mean size reflects the energy level of transporting currents, with coarser sands suggesting proximity to source and higher competence flows (Pettijohn, 1975). Sorting values (σϕ) indicate that 60% of the samples are poorly sorted, 30% moderately sorted, and 10% well sorted (Table 2). Poor sorting reflects fluctuating energy conditions and rapid deposition, possibly linked to channelised fluvial discharge and proximal alluvial inputs (Krumbein & Sloss, 1963). Similar results have been documented in fluvial-dominated successions in the Benue Trough (Nwajide, 2013; Obi et al., 2014). Skewness values range from negatively skewed to near-symmetrical (Table 2). About 40% of the samples are negatively skewed, suggesting coarser-tail dominance, while 40% are coarse-skewed and 20% fine-skewed. Negative skewness indicates selective removal of fines by traction currents, a common feature in high-energy fluvial–shoreface settings (Friedman, 1961). Kurtosis values reveal 20% leptokurtic, 40% platykurtic, 10% very platykurtic, and 30% mesokurtic distributions (Table 2). While kurtosis generally contributes limited geological significance (Pettijohn, 1975), the predominance of platykurtic curves reflects broad, flat distributions typical of variable depositional regimes where both traction and suspension processes operate.

Table 2. Particle size distribution and statistical parameters of Ajali Formation samples

Sample		Mean		Standard deviation		Skewness		Kurtosis
RIY 1A	0.59	Coarse grained	1.21	Poorly sorted	-0.23	Negatively skewed	1.17	Leptokurtic
RIY 1B	0.89	Coarse grained	0.50	Well sorted	-0.14	Negatively skewed	1.15	Leptokurtic
RIY 1C	1.20	Medium grained	0.75	Medium sorted	0.27	Strongly fine skewed	0.61	Very platykurtic
RIY 1D	1.02	Coarse grained	1.03	Poorly sorted	-0.12	Negatively skewed	0.70	Platykurtic
RIY 1E	1.22	Medium grained	1.01	poorly sorted	0.25	Positively skewed	0.93	Mesokurtic
RIY 3E	1.23	Medium grained	1.01	Medium sorted	-0.59	Strongly coarse skewed	0.95	Mesokurtic
RIY 3B	0.61	Coarse grained	1.13	Poorly sorted	-0.10	Strongly coarse skewed	0.80	Platykurtic
RIY 3D	1.01	Coarse grained	0.90	Medium sorted	-0.34	Strongly coarse skewed	0.83	Platykurtic
RIY 4A	0.77	Coarse grained	1.35	Poorly sorted	0.87	Strongly fine skewed	0.85	Platykurtic
RIY 4B	0.80	Coarse grained	1.03	Poorly sorted	-0.12	Negatively skewed	0.95	Mesokurtic

4.2.3 Bivariate Plots

The bivariate plot of mean grain size against sorting (after Moiola & Weiser, 1968) shows that 100% of the samples fall within the fluvial field (Fig. 9). This reinforces the interpretation of Ajali Sandstone as fluvial-dominated, consistent with earlier works that describe it as a high-energy braided fluvial system with localised marine influence (Nwajide, 2013; Akande et al., 2021).

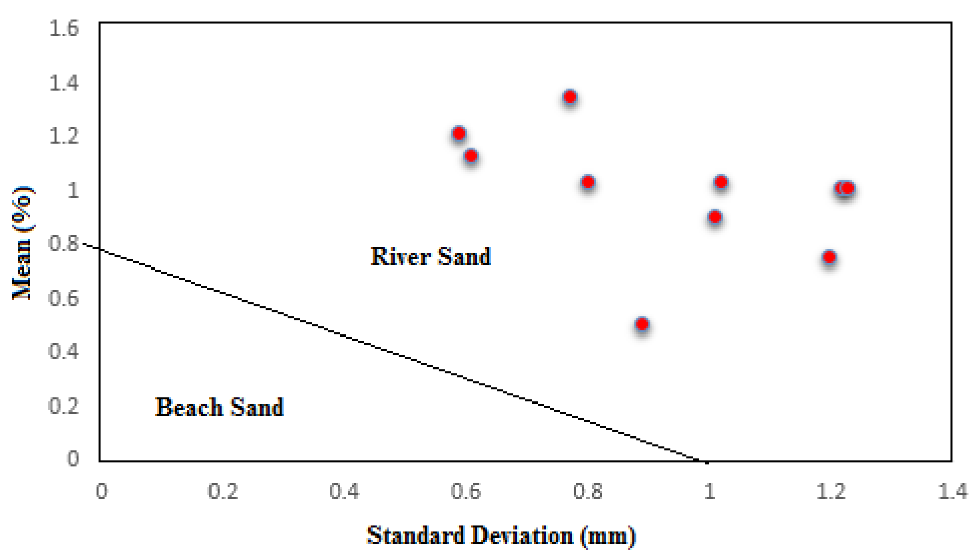

Figure 9: Grain-size bivariate plot of mean vs sorting showing river and beach fields (after Moiola & Weiser, 1968).

4.2.4 Linear Discriminant Function (LDF) Analysis

Discriminant function analysis (Sahu, 1964) was applied to further constrain depositional settings using mean size, sorting, skewness, and kurtosis. The Y1–Y2 plot (Fig. 10a) reveals that 95% of Ajali samples plot within the beach/shallow marine field, while 5% fall in the aeolian domain. Similarly, the Y2–Y3 plot (Fig. 10b) indicates that 55% of the samples align with fluvial–deltaic processes, while 45% suggest deposition under turbidity currents (Table 3). These results highlight the complex interplay of depositional processes, where the Ajali Sandstone records alternating high-energy braided fluvial inputs and nearshore reworking, while the finer-grained Mamu Formation reflects quieter floodplain, swamp, and deltaic conditions.

Table 3. Linear Discriminant Function classification of Ajali Formation samples (after Sahu, 1964)

S/N	SAMPLE ID	Y1	REMARK	Y2	REMARK	Y3	REMARK
1	RIY 1A	7.31	Beach	122.00	Shallow agitated marine (subtidal)	-11.25	Fluvial Deltaic
2	RIY 1B	1.42	Beach	50.52	Shallow agitated marine (subtidal)	-1.16	Shallow marine
3	RIY 1C	-0.78	Beach	72.02	Shallow agitated marine (subtidal)	-5.93	Shallow marine
4	RIY 1D	2.86	Beach	97.43	Shallow agitated marine (subtidal)	-8.57	Fluvial Deltaic
5	RIY 1E	1.90	Beach	107.01	Shallow agitated marine (subtidal)	-9.60	Fluvial Deltaic
6	RIY 3E	3.30	Beach	86.00	Shallow agitated marine (subtidal)	-4.75	Shallow marine
7	RIY 3B	5.21	Beach	105.91	Shallow agitated marine (subtidal)	-10.54	Fluvial Deltaic
8	RIY 3D	2.90	Beach	80.00	Shallow agitated marine (subtidal)	-5.21	Shallow marine
9	RIY 4A	5.00	Beach	164.50	Shallow agitated marine (subtidal)	-20.09	Fluvial Deltaic
10	RIY 4B	4.30	Beach	97.29	Shallow agitated marine (subtidal)	-8.59	Fluvial Deltaic
			B=100%		SAM = 100%		FD = 60% SM = 40%

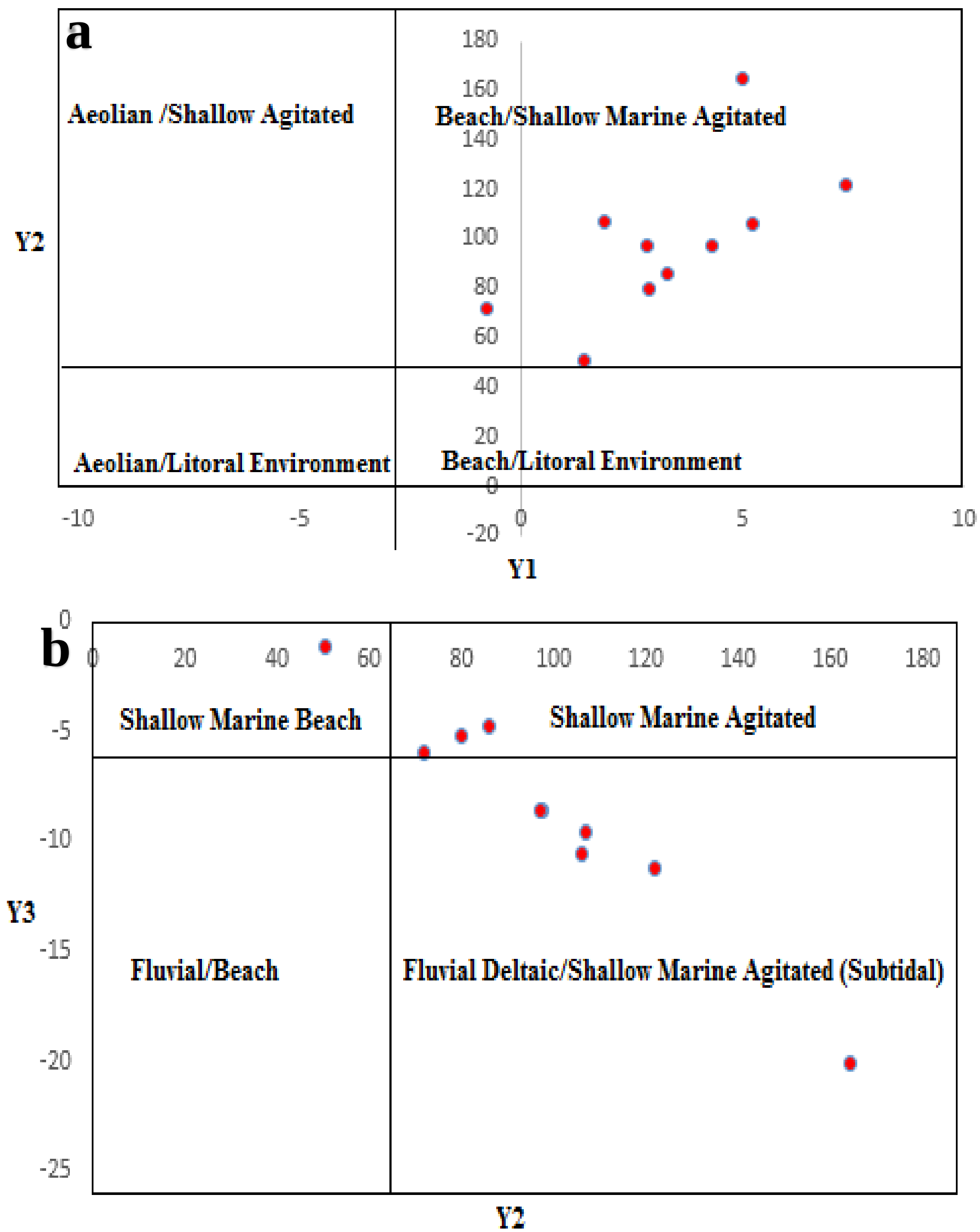

Figure 10. Linear Discriminant Function scatter plots (a) Y1 vs Y2, (b) Y2 vs Y3 for Ajali Formation in Iyale

4.2.5 CM Pattern Analysis

Passega's CM diagrams (Passega, 1957; 1964) were constructed to interpret transport mechanisms. Results show that 65.2% of samples plot within the rolling field, while 34.8% fall within the bottom-suspension and rolling fields (Fig. 11). The predominance of rolling suggests tractional bedload transport under turbulent fluvial conditions, whereas the bottom-suspension group indicates combined traction–suspension processes during waning flow. Similar CM patterns have been reported for deltaic–fluvial complexes in West Africa (Visher, 1969; Rajganapathi et al., 2012; Ojo & Akande, 2020).

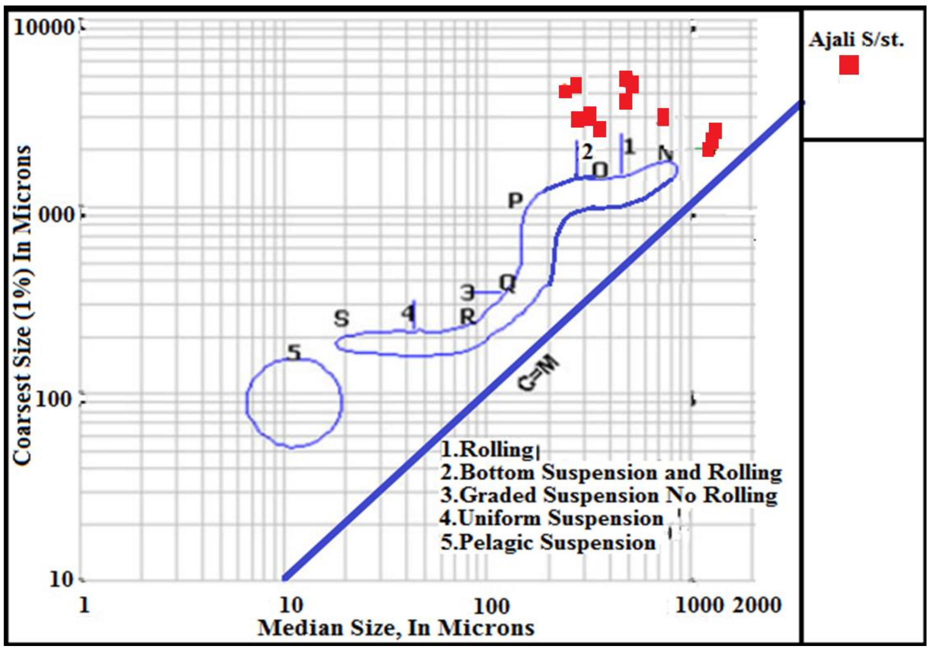

Figure 11. CM diagram for Ajali Formation sandstones in Iyale area (after Passega, 1957, 1964)

4.2.6 Integrated Palaeoenvironmental Implications

The granulometric data collectively suggest that the Ajali Sandstone in Iyale was deposited predominantly in a high-energy fluvial to shallow marine environment, consistent with braided river systems grading into coastal settings. The dominance of medium–coarse grains, poor sorting, negative skewness, and CM patterns indicate rapid deposition from turbulent currents with limited reworking. The occasional marine overprint, revealed by LDF plots, points to shoreline proximity during deposition. In contrast, the Mamu Formation exposures in Agbenema display finer-grained lithologies, better sorting in places, and positive skewness, consistent with floodplain, swamp, and lower-energy deltaic sub-environments. This conforms with the established model of Ajali as a fluvial-dominated sandstone and Mamu as paralic/coastal plain deposits (Nwajide, 2013; Obi et al., 2014; Akande et al., 2021). Thus, granulometric analysis corroborates field observations and facies descriptions, supporting a palaeoenvironmental reconstruction in which the Ajali Sandstone records proximal braided fluvial systems transitioning into shallow marine shoreface deposits, while the Mamu Formation reflects paralic to swamp-dominated settings within the Northern Anambra Basin.

4.3 Petrography and Sandstone Classification

Petrographic analysis provides insights into sandstone maturity, provenance, and depositional settings. Modal composition of Ajali Sandstone (Table 4) indicates that the sandstones are dominated by quartz (83–96%; mean = 91.2%), with subordinate feldspar (1–11%; mean = 3.2%) and rock fragments (3–8%; mean = 5.5%). According to Pettijohn (1975) and Folk (1980), 90% of the samples classify as quartz arenites, while the remaining 10% fall within the subarkose field (Fig. 12). This compositional trend suggests a high degree of textural and mineralogical maturity. The prevalence of monocrystalline and polycrystalline quartz grains (Figs. 13a-f) reflects intense chemical weathering and sediment recycling, likely sourced from continental blocks and reworked sedimentary rocks. The low feldspar content points to substantial alteration during transport and diagenesis, whereas the moderate rock fragment content suggests derivation from granitoid and metamorphic terranes (Dickinson & Suczek, 1979; Baiyegunhi et al., 2017). The relatively high quartz content (>90%) in samples such as RIY1A, RIY3D, and RIY4B may signify reworking under fluvial processes or strong sediment recycling within a stable passive margin setting (Dickinson, 1985). Variations in quartz proportions between samples imply subtle shifts in provenance or depositional environments. These findings corroborate earlier interpretations of the Ajali Sandstone as products of braided river systems prograding into shallow marine settings during the Campanian–Maastrichtian regression (Reyment, 1965; Nwajide, 2013). Collectively, the petrographic classification demonstrates that the Ajali Sandstone is dominated by quartz arenites with subordinate subarkoses, reflecting deposition under stable cratonic to passive margin conditions, controlled by long transport distances, recycling, and weathering processes.

Table 4. Modal composition of Ajali Sandstone facies

S/N	Sample ID	Quartz	Feldspar (F)	Rock (RF)	Fragment	F+RF
1	RIY 1A	96	1	3		4
2	RIY 1B	91	3	6		9
3	RIY 1C	90	3	7		10
4	RIY 1D	91	2	7		9
5	RIY 1E	83	11	6		17
6	RIY 3E	95	2	3		5
7	RIY 3B	90	3	7		10
8	RIY 3D	96	1	3		4
9	RIY 4A	90	2	8		10
10	RIY 4B	95	2	3		5
	Average	91.20	3.2	5.5		8.8

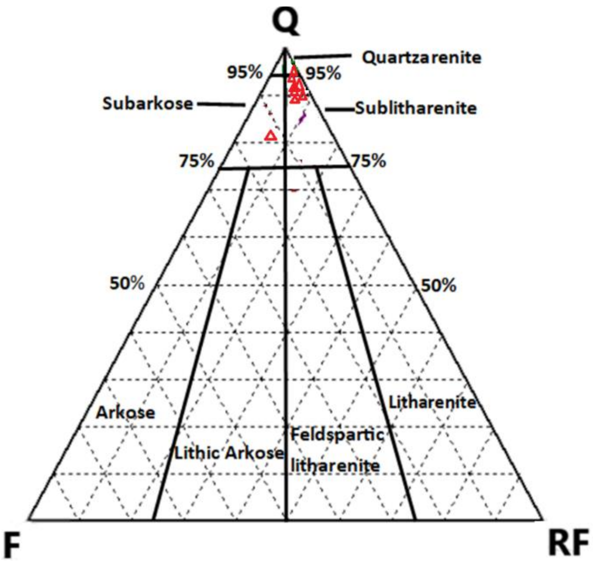

Figure 12. Sandstone classification of Ajali Sandstone (after Folk, 1980)

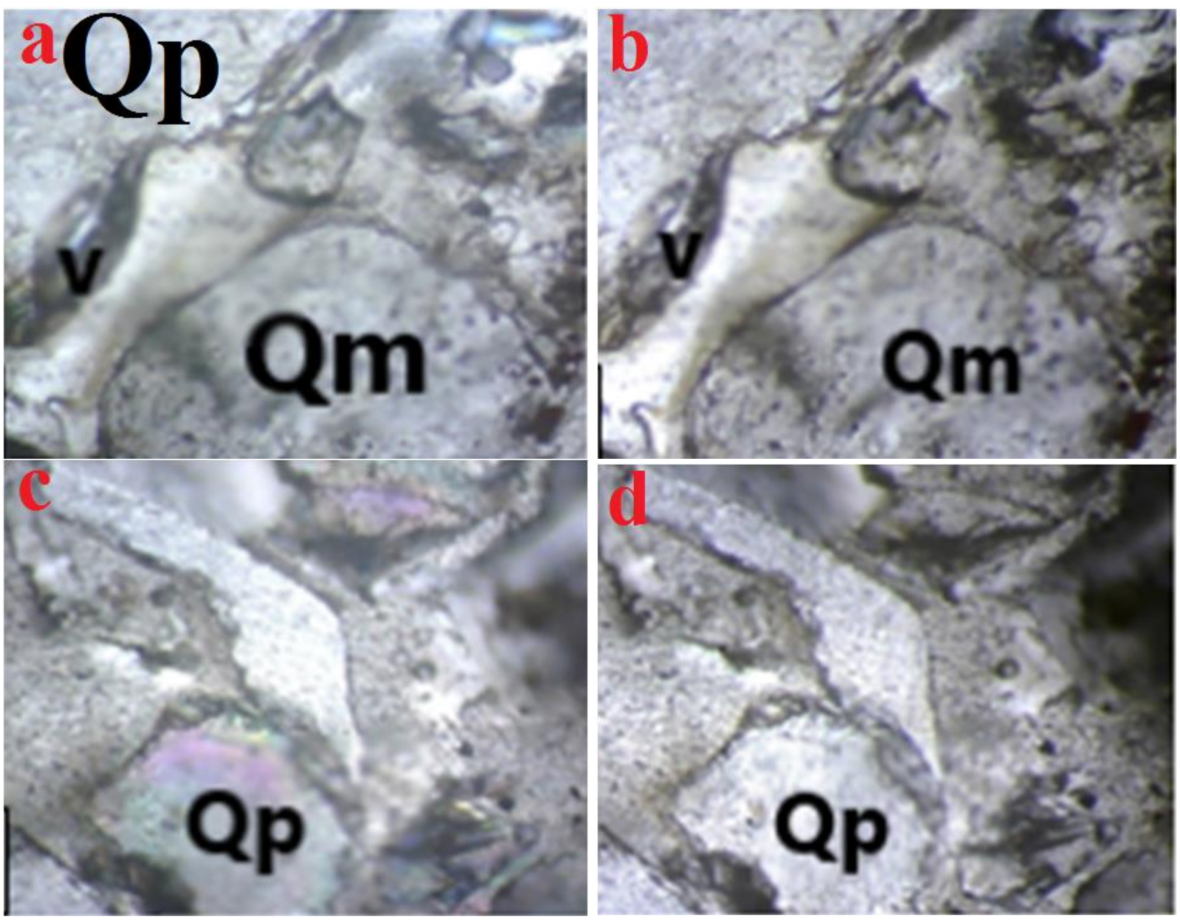

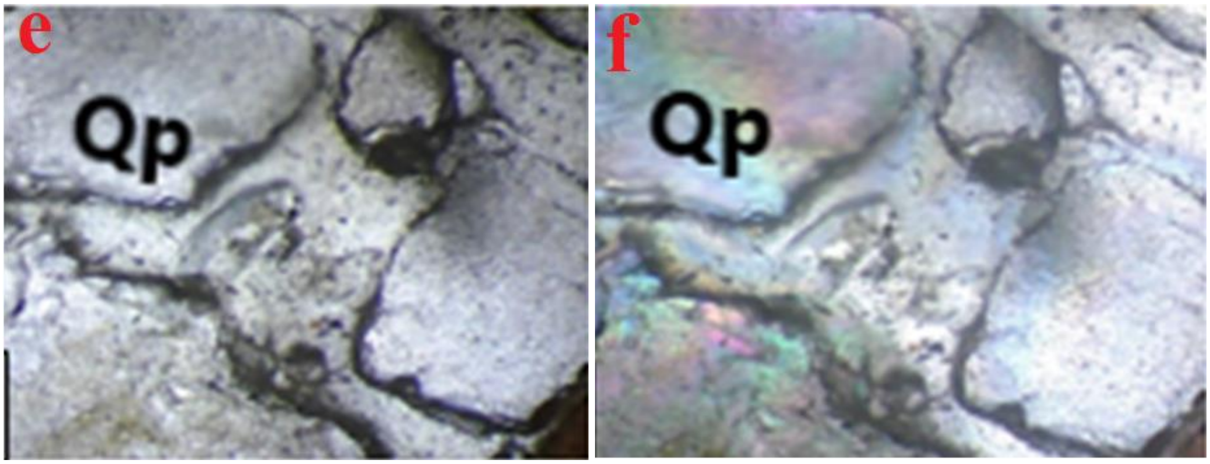

Figure 13. (a-f) Photomicrographs showing monocrystalline and polycrystalline quartz (XPL and PPL views).

4.4 Heavy Minerals

Heavy mineral analysis further constrains provenance and sediment recycling processes. The assemblages from Ajali Sandstone at Iyale and environs (RIY1, RIY4, RIY5, RIY7, RIY11) include zircon, tourmaline, rutile, staurolite, apatite, garnet, magnetite, and hematite (Table 5; Figs. 14a–b). Opaque minerals constitute ~11.4%, while non-opaques dominate, with zircon (42.2%), tourmaline (30.8%), staurolite (5.7%), rutile (4.7%), apatite (4.7%), and garnet (0.5%). The calculated ZTR index averages 87.7%, indicating mineralogical submaturity but strong enrichment in ultrastable phases. The abundance of well-rounded zircon and tourmaline, with evidence of overgrowths, suggests derivation from multicycle sedimentary sources (Potter & Pettijohn, 1977; Morton & Hallsworth, 1994). The presence of rutile, typically sourced from high-grade metamorphic rocks (Force, 1980), supports inputs from metamorphic terranes. Integration with palaeocurrent data implies that the Santonian Okigwe–Abakaliki uplift served as the principal sediment source, with minor contributions from the Oban Massif basement complex. The Cameroon basement complex, by contrast, appears to have had negligible input, likely due to its distance and the shielding effect of the Santonian uplift. This provenance model aligns with previous reconstructions of the Northern Anambra Basin, where foreland-controlled sediment dispersal systems redistributed clastic input from uplifted basement and recycled sedimentary terranes (Nwajide, 2013; Obi et al., 2020). Thus, the heavy mineral assemblages of Ajali Sandstone reinforce petrographic evidence of multicycle sediment derivation, intense weathering, and recycling, within a tectonically stable passive margin setting.

Table 5. Relative abundances of heavy mineral assemblages in Ajali Sandstone

Sample Location	Zircon	Tourmaline	Rutile	Apatite	Staurolite	Garnet	Total	ZRT	ZRT Index (%)	Opaque
RIY1	25.0	21.0	3.0	1.0	5.0	1.0	55.0	49.0	89.09	8.0
RIY4	21.0	14.0	2.0	2.0	1.0	1.0	41.0	37.0	90.24	5.0
RIY5	20.0	16.0	3.0	5.0	3.0		47.0	39.0	82.98	6.0
RIY7	22.0	13.0	2.0	2.0	1.0	1.0	41.0	37.0	90.24	6.0
RIY11	23.0	14.0	2.0	2.0	3.0		44.0	39.0	88.64	5.0
Total	89.0	65.0	10.0	10.0	12.0	1.0			350.95	24.0
% composition	42.2	30.8	4.7	4.7	5.7	0.47				

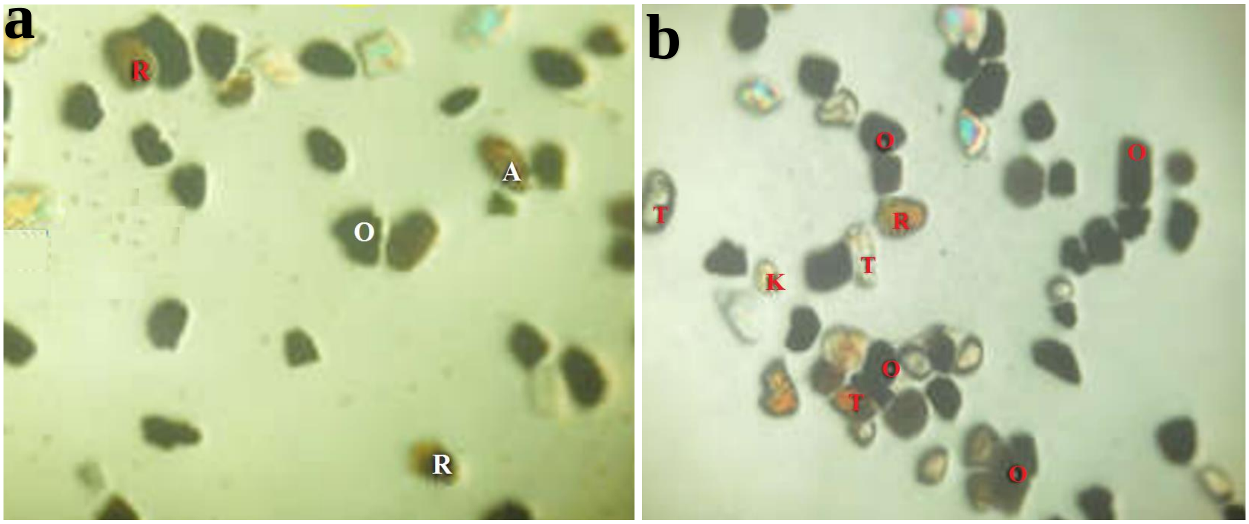

Figure 14. Photomicrographs of heavy minerals (plane polarised light, 30×). Z=Zircon, R=Rutile, T=Toumaline, G=Garnet, S=Staurolite, K=Kyanite, O=Opaque, A= Apatite

5. *Conclusions*

This study integrates field, granulometric, petrographic, and heavy mineral analyses to reconstruct the facies architecture and depositional environments of the Ajali Sandstone and Mamu Formation in the northern Anambra Basin. The Ajali Sandstone exhibits medium–coarse grained, poorly sorted quartz arenites, with negative skewness, platykurtic curves, and traction-dominated CM patterns. These features, combined with cross-bedding, flaser structures, and Skolithos burrows, confirm deposition in high-energy fluvial–tidal channels and intertidal flats with periodic marine influence. Petrography and heavy mineral assemblages (zircon, tourmaline, rutile) indicate multicycle sediment recycling and derivation from uplifted basement and sedimentary terranes. Conversely, the Mamu Formation is dominated by finer-grained clay, siltstone, and shale facies, with root traces, plant debris, and ferruginised horizons, reflecting floodplain to prodelta conditions under fluctuating redox states. Together, these successions capture the dynamic interplay of Late Cretaceous transgressive–regressive cycles, where braided fluvial systems prograded into coastal plain and shallow marine settings.

Acknowledgments

This paper is based on part of the MSc thesis of the first author under the supervision of the second and third authors.

References

Adamu, M.L., Rufai, A., Atabo, N.O. and Alege, T.S. (2017). Sedimentology and Depositional Environment of the Mid-MaastritchtianAjali Sandstone in Idah and Environs, Northern Anambra Basin, Northcentral Nigeria, *Journal of Applied Geology and Geophysics,* (6)1, 38-51.

Adamu, M.L., Hamza, H., Hamidu, I. and Obaje, N.G. (2018a).Sedimentology and Stratigraphy of the Campano-Maastritchtian Succession, Northeast of Idah Town, northern Anambra Basin, *DJOSTER,* 7(1), 127-153.

Adamu, L.M., Odoma, A.N., Ibrahim, M.M., Umar, U.O. and Alege, T. S. (2018b). Lineament Analysis and Structural Evolution of Ajaka and Environs, Northern Anambra Basin, *DJOSTER*, 7(2), 110-123.

Adamu M.L., Ayuba, R. and Alege, T.S. (2018c). Sedimentology and Depositional Environments of the MaastrichtianMamu Formation, Northern Anambra Basin, Nigeria, *Advances in Applied Science Research*, 9(2), 53-68.

Adamu, L.M., Obaje, N.G., Ngozi, O.P. and Umar, U.M. (2020). Integrated Geochemical and Multivariate Statistical Examination of Source Rocks in the Sokoto and Anambra Basins, Nigeria: Implications for Hydrocarbon Prospectivity, *Petroleum Science and Engineering,* 4(2), 39-50.

Adamu, L.M., Obaje, N.G., Ayuba, R., Kovona, M.T., Adesino, D.A., and Etukudo, N.J. (2022a). Litho-Bio Facies analysis and Systematic Paleontology of Sediments in Amansiodo-1 Well, Anambra Basin, Southeastern Nigeria. *Earth Sciences*, 11(3), 96-108. doi:10.11648/j.earth.20221103.16.

Adamu, L.M., Andongma, W.T., Jiriko, N.G., Mazadu, D.B., Shinkafi, F., and Mohammed, D.A. (2022b). A bivariate statistical analysis for coal exploration within parts of the Anambra Basin in Nigeria, *Spatial Information Research, Springer*, https://doi.org/10.1007/s41324-022-00440-x

Adamu, L.M., Obaje, N.G., Adeoye, J.A., Oladimeji, R.G., and Yusuf, I. (2024). Trans-Saharan seaway connection between the south Atlantic and the Tethys Sea during the Coniacian – Turonian: Evidence from bibliographical synthesis, field mapping, and seismic interpretation, *Geosystems and Geoenvironment, Elsevier*, 3(2024) 100243.

Agagu, O. K., Fayose, E. A., & Petters, S. W. (1985). Stratigraphy and sedimentation in the Senonian Anambra Basin of southeastern Nigeria. *Journal of Mining and Geology, 22*(1–2), 25–36.

Akande, S. O., & Erdtmann, B. D. (1998). Burial metamorphism (thermal maturity) of the Cretaceous sediments in the southern Benue Trough and Anambra Basin, Nigeria. *American Association of Petroleum Geologists Bulletin, 82*(6), 1191–1206.

Akande, S. O., Ojo, O. J., & Adekeye, O. A. (2021). Sedimentology and depositional environments of the Campanian–Maastrichtian formations in the Anambra Basin, Nigeria. *Journal of African Earth Sciences, 174*, 104086. https://doi.org/10.1016/j.jafrearsci.2020.104086

Alege, O. A., Obaje, N. G., Umar, A. F., & Yusuf, I. (2023). Stratigraphic framework and petroleum system implications of the Anambra Basin, Nigeria. *Marine and Petroleum Geology, 149*, 106024. https://doi.org/10.1016/j.marpetgeo.2023.106024

Allen, J. R. L. (1984). *Sedimentary structures: Their character and physical basis* (Vol. 2). Elsevier.

Anyiam, U. O., Mode, A. W., & Ekweozor, C. M. (2015). Depositional environment and sequence stratigraphy of the Campanian–Maastrichtian succession in Anambra Basin, southeastern Nigeria. *Journal of African Earth Sciences, 111*, 1–12.

Baiyegunhi, C., Liu, K., Gwavava, O., & Oloniniyi, T. L. (2017). Provenance and tectonic setting of sandstones in the Karoo Supergroup, Lower Beaufort Group, Main Karoo Basin, South Africa. *Acta Geochimica, 36*(4), 669–687. https://doi.org/10.1007/s11631-017-0181-5

Blott, S. J., & Pye, K. (2001). Gradistat: A grain size distribution and statistics package for the analysis of unconsolidated sediments. *Earth Surface Processes and Landforms, 26*(11), 1237–1248.

Boggs, S. (1995). *Principles of sedimentology and stratigraphy* (2nd ed.). Prentice Hall.

Boggs, S. (2012). *Principles of sedimentology and stratigraphy* (5th ed.). Pearson Education.

Dickinson, W. R. (1985). Interpreting provenance relations from detrital modes of sandstones. In G. G. Zuffa (Ed.), *Provenance of arenites* (pp. 333–361). Springer.

Dickinson, W. R., & Suczek, C. A. (1979). Plate tectonics and sandstone compositions. *American Association of Petroleum Geologists Bulletin, 63*(12), 2164–2182.

Dim, C. I., Mode, A. W., Anyiam, U. O., & Umeji, O. P. (2018). Depositional environments and sequence stratigraphy of the Mamu Formation in parts of the Anambra Basin, southeastern Nigeria. *Journal of African Earth Sciences, 143*, 254–266.

Erepamo, O., Akande, S. O., & Obaje, N. G. (2022). Sedimentological and palaeoenvironmental analysis of the Nsukka Formation, Anambra Basin, Nigeria. *Journal of African Earth Sciences, 190*, 104569.

Fatoye, F. B., & Yomi, A. O. (2013). Depositional environment and reservoir characteristics of the Ajali Sandstone, Anambra Basin, Nigeria. *International Journal of Scientific & Technology Research, 2*(8), 174–180.

Folk, R. L. (1980). *Petrology of sedimentary rocks*. Hemphill Publishing Company.

Folk, R. L., & Ward, W. C. (1957). Brazos River bar: A study in the significance of grain size parameters. *Journal of Sedimentary Petrology, 27*(1), 3–26.

Force, E. R. (1980). The provenance of rutile. *Journal of Sedimentary Petrology, 50*(2), 485–488.

Friedman, G. M. (1961). Distinction between dune, beach, and river sands from their textural characteristics. *Journal of Sedimentary Petrology, 31*(4), 514–529.

Friedman, G. M. (1979). Differences in size distributions of populations of particles among sands of various origins. *Sedimentology, 26*(1), 3–32.

Guiraud, R., & Bosworth, W. (1997). Senonian basin inversion and rejuvenation of rifting in Africa and Arabia: Synthesis and implications to plate-scale tectonics. *Tectonophysics, 282*(1–4), 39–82.

Krumbein, W. C., & Sloss, L. L. (1963). *Stratigraphy and sedimentation* (2nd ed.). Freeman.

Magoon, L. B., & Dow, W. G. (1994). *The petroleum system—from source to trap*. American Association of Petroleum Geologists Memoir 60.

Miall, A. D. (1996). *The geology of fluvial deposits: Sedimentary facies, basin analysis, and petroleum geology*. Springer.

Mode, A. W., Anyiam, U. O., Dim, C. I., & Umeji, O. P. (2019). Sedimentology and depositional environments of the Mamu Formation in parts of the Anambra Basin, southeastern Nigeria. *Journal of African Earth Sciences, 150*, 223–234.

Moiola, R. J., & Weiser, D. (1968). Textural parameters: An evaluation. *Journal of Sedimentary Petrology, 38*(1), 45–53.

Morton, A. C., & Hallsworth, C. R. (1994). Identifying provenance-specific features of detrital heavy mineral assemblages in sandstones. *Sedimentary Geology, 90*(3–4), 241–256.

Morton, A. C., & Hallsworth, C. R. (1999). Processes controlling the composition of heavy mineral assemblages in sandstones. *Sedimentary Geology, 124*(1–4), 3–29.

Nwajide, C. S. (2013). *Geology of Nigeria's sedimentary basins*. CSS Bookshops Ltd.

Nwajide, C. S., & Reijers, T. J. A. (1996). Geology of the southern Anambra Basin. *Nigeria Association of Petroleum Explorationists Bulletin, 11*(1), 23–37.

Obaje, N. G. (2009). *Geology and mineral resources of Nigeria*. Springer.

Obaje, N. G., Attah, D. O., Opeloye, S. A., & Moumouni, A. (2004). Geochemical evaluation of the hydrocarbon prospects of sediments in the Anambra Basin, SE Nigeria. *Nigerian Association of Petroleum Explorationists Bulletin, 17*(1), 1–16.

Obaje, N. G., Balogun, O. J., Yusuf, I., & Omada, J. I. (2020). Sedimentology and palaeoenvironmental implications of Maastrichtian formations in northern Anambra Basin, Nigeria. *Journal of African Earth Sciences, 169*, 103900.

Obaje, N. G., Okoro, E. U., & Moumouni, A. (2013). Petroleum prospectivity of Nigeria's inland basins: From the Chad Basin to the Bida Basin. *Journal of Petroleum Exploration and Production Technology, 3*(2), 59–70.

Obaje, N. G., Wehner, H., Scheeder, G., Abubakar, M. B., & Jauro, A. (1999). Hydrocarbon prospectivity of Nigeria's inland basins: From the Chad Basin to the Bida Basin. *Nigerian Association of Petroleum Explorationists Bulletin, 14*(1), 37–50.

Obi, G. C., Okogbue, C. O., & Nwajide, C. S. (2014). Facies architecture and depositional environments of Campanian–Maastrichtian Anambra Basin sediments, southeastern Nigeria. *Sedimentary Geology, 299*, 1–14.

Obi, G. C., Okogbue, C. O., Mode, A. W., & Dim, C. I. (2020). Facies analysis and palaeoenvironmental evolution of the Campanian–Maastrichtian Ajali Sandstone, Anambra Basin, Nigeria. *Journal of African Earth Sciences, 164*, 103722.

Odumoso, P. E., Akande, S. O., & Erdtmann, B. D. (2013). Geochemistry and depositional environment of the Nkporo Shale and Mamu Formation in the Anambra Basin, SE Nigeria. *Journal of African Earth Sciences, 80*, 10–22.

Ojo, O. J., & Akande, S. O. (2020). Granulometric analysis and depositional environment of sandstones in the Bida Basin, Nigeria. *Journal of African Earth Sciences, 166*, 103813.

Ogumagbe, E., Omada, J. I., & Yusuf, I. (2022). Stratigraphic evolution and petroleum system elements of the Anambra Basin, southeastern Nigeria. *Marine and Petroleum Geology, 144*, 105800.

Passega, R. (1957). Texture as characteristic of clastic deposition. *American Association of Petroleum Geologists Bulletin, 41*(9), 1952–1984.

Passega, R. (1964). Grain-size representation by CM patterns as a geological tool. *Journal of Sedimentary Petrology, 34*(4), 830–847.

Pemberton, S. G., & MacEachern, J. A. (1997). The ichnological signature of storm deposits: The use of trace fossils in event stratigraphy. In C. P. Brett & G. C. Baird (Eds.), *Paleontological Society Papers, 2* (pp. 73–109).

Pettijohn, F. J. (1975). *Sedimentary rocks* (3rd ed.). Harper & Row.

Potter, P. E., & Pettijohn, F. J. (1977). *Paleocurrents and basin analysis* (2nd ed.). Springer.

Rajganapathi, R., et al. (2012). Grain-size characteristics and depositional environments of the Palar River sediments, Tamil Nadu, India. *Journal of Geological Society of India, 80*(3), 389–398.

Reading, H. G. (1996). *Sedimentary environments: Processes, facies and stratigraphy* (3rd ed.). Blackwell Science.

Reineck, H. E., & Singh, I. B. (1980). *Depositional sedimentary environments* (2nd ed.). Springer-Verlag.

Reyment, R. A. (1965). *Aspects of the geology of Nigeria: The stratigraphy of the Cretaceous and Cenozoic deposits*. Ibadan University Press.

Sahu, B. K. (1964). Depositional mechanisms from the size analysis of clastic sediments. *Journal of Sedimentary Petrology, 34*(1), 73–83.

Tucker, M. E. (1996). *Sedimentary rocks in the field* (2nd ed.). Wiley-Blackwell.

Visher, G. S. (1969). Grain-size distributions and depositional processes. *Journal of Sedimentary Petrology, 39*(3), 1074–1106.

Wentworth, C. K. (1922). A scale of grade and class terms for clastic sediments. *Journal of Geology, 30*(5), 377–392.

Whiteman, A. J. (1982). *Nigeria: Its petroleum geology, resources and potential* (Vol. 1 & 2). Graham & Trotman.

Wright, J. B., Hastings, D. A., Jones, W. B., & Williams, H. R. (1985). *Geology and mineral resources of West Africa*. Allen & Unwin.

Yusuf, I., Obaje, N. G., & Omada, J. I. (2023). Sedimentology and palaeoenvironmental reconstruction of Late Cretaceous deposits in the northern Anambra Basin, Nigeria. *Journal of African Earth Sciences, 199*, 104879.

Zaborski, P. M. (2000). The Cretaceous and Palaeogene history of the Nigerian sector of the Iullemmeden Basin (West Africa). *Geological Society, London, Special Publications, 153*(1), 487–504.